JOURNAL OF MATERIALS SCIENCE 33 (1998) 4813–4819

Hydrogen-inducing nanovoids in thin crystals of 310 stainless steel

Q. Z. CHEN, G. H. ZHOU, Y. Z. HUANG, W. Y. CHU
Department of Materials Physics, University of Science and Technology Beijing, Beijing 100083, China

Hydrogen-inducing nanovoids in hydrogenated 310 stainless steel was investigated by *in situ* tension in TEM. It was found experimentally that hydrogen-induced cracking happened through nanovoid nucleation and then quasi-cleavage along {1 1 1} planes when C_H is high. Otherwise, in the case of low C_H, hydrogen-enhanced ductile fracture through hydrogen-induced microvoid nucleation, growth and connection. A new model was proposed based on the present experiments. Dislocations breakaway from defect atmospheres and move away from the DFZ, leaving vacancy and hydrogen clusters along {1 1 1} planes. Hydrogen tends to combine with vacancy clusters and initiate nanovoids along {1 1 1} planes. Dense nanovoids connect each other, resulting in brittle cracking. Scattered nanovoids grow into microvoids or even macrovoids, leading to ductile fracture.

1. Introduction

Many experiments [1–5] have shown that hydrogen-induced cracking (HIC) in intermediate- and low-strength steels involved the mechanism of hydrogen-enhancing voids. There are two views on hydrogen-promoting voids. Thompson *et al.* [6–8] suggested that hydrogen-promoted void growth and interlinkage, but it had almost no effect on void nucleation. On the other hand, Kwon and Asaro [9] concluded that hydrogen enhanced void nucleation at average-sized carbide particles by reducing the critical interfacial strength. However some experiments indicate that second phases may not be essential for initiation of voids [10, 11]. Lee and Bernstein [3] found that hydrogen-enhanced void nucleation along the characteristic slip bands. The present investigation is aimed at how hydrogen promotes voids that induce HIC in 310 stainless steel.

HIC could occur in hydrogenated stable austenitic stainless steel [5, 13–14], which had no relation with martensitic transformation [12–13]. Macro experiments on stable stainless steels show that hydrogen enhanced ductile failure by promoting voids when hydrogen concentration C_H was low and applied stress strength factor K_{ap} was high, resulting in dimple fracture [12]. Otherwise hydrogen-induced brittle failure when C_H was high and K_{ap} was low, resulting in quasi-cleavage fracture [12]. The microvoids (or microcracks) that were observed in the above-mentioned macro-investigations, even in TEM observations [5], were developed quite away from the earliest initiation stage and might not exactly reflect their initiation mechanism. One objective of the present investigation is to observe, by *in situ* tension in TEM, the effect of hydrogen on nanovoid nucleation while elongating thin foils of hydrogen-charged 310 stainless steel, as well as the different mechanisms of HIC when hydrogen concentrations are varied.

Obviously, the vacancy-hydrogen interactions can be useful for interpretation of HIC. Chen *et al.* [15] found that dislocation-free zones (DFZs) played an important role in failure. They are beneficial to nanocrack nucleation. The highly concentrated stresses induced supersaturation of vacancies in DFZs, where the diffusion and enrichment of vacancies initiated nanovoids. The calculation by Bockris and Subramanyam [16] indicates that a high-stress concentration enriches hydrogen in the precharged specimen. Recent theoretical and experimental work [17, 18] has predicted and confirmed that the vacancy-interstitial interactions can lead to the formation of much higher vacancy concentrations in metals than are observed in the interstitial-free materials. The other objective of this paper is to propose a model of void initiation by cooperation of hydrogen and vacancies in highly concentrated stress fields.

2. Experimental procedures

Stable austenitic stainless steel of type 310 was used, considering that not only could HIC happen without involving ε-martensite in it [12–13], but also the diffusion coefficient of hydrogen D_H is quite small (about 10^{-12} cm^2/s) [19]. Therefore, hydrogen can stay in this type of thin foil for a longer time than in ferritic steels (D_H is about 10^{-5} cm^2/s [19]). The testing time must be so short that there is sufficient hydrogen to initiate cracking in thin foils during *in situ* elongation. The variation of hydrogen concentration with testing time is estimated in Appendix A.

The composition of the present 310 stainless steel, the heat treatments and the polishing solutions are the

same as those in the earlier work [15]. TEM foils were prepared from a strip of 0.2 mm. First, the sheet was thinned to about 50 μm by chemical polishing. Then, the specimens were cathodically charged at room temperature for at least 50 h in a 0.5 M H_2SO_4 solution containing 250 mg As_2O_3 per liter. A platinum counter electrode and a current density of 0.5 A/cm^2 were used. The hydrogen concentration was measured, by degassing at 1000 °C, to be more than 200 ppm. Finally, the precharged specimens were electropolished. *In situ* elongation was performed in JEM 100-CX immediately after hydrogenating and electropolishing.

The present *in situ* observation was carried under constant displacement for the following reasons. First, the details of initiation could be caught under such a relatively stable condition. Second, the applied-stress σ_{ap} can be smaller than the yield-stress σ_y when constant displacement was kept, and HIC can be observed.

The ductile cracking of the hydrogen-free specimen, which was prepared by ion milling, was observed first under constant displacement so as to compare it with that of the hydrogenated specimen.

3. Results

3.1. Crack initiation in the hydrogen-free specimen

Cracking took place when a region was loaded sufficiently. When keeping constant displacement for a while, the main crack stopped propagating, and no deformation was observed in the whole specimen except in the zone ahead of the crack tip. This indicated that the macro-applied stress σ_{ap} had been smaller than the yield-stress σ_y. In the zone ahead of the crack tip, however, cracking was still developing slowly, as shown in Fig. 1. The voids developed slowly [it took about 30 m from Fig. 1a to c], as in the case of creeping where vacancies played an important role. In the zone AB, no dislocation was observed by tilting the specimen extensively. Two factors may be responsible for DFZs. First, mechanical equilibrium needs such a DFZ to exist [15]. Second, a dislocation may not be supported in such a sample thickness [10].

In Fig. 2, the effect of vacancies on void formation was more obvious when constant displacement was kept for a long time. Two nanovoids formed very slowly just ahead of the crack tip, as arrowed in Fig. 2b and c. It is vacancies that initiated the two nanovoids. Chen *et al.* ascribed this phenomenon to vacancy supersaturation induced by stress concentration in the DFZ ahead of the crack tip [15]. It is imaginable that hydrogen will enhance the nucleation of nanovoids and stabilize them in hydrogenated specimens.

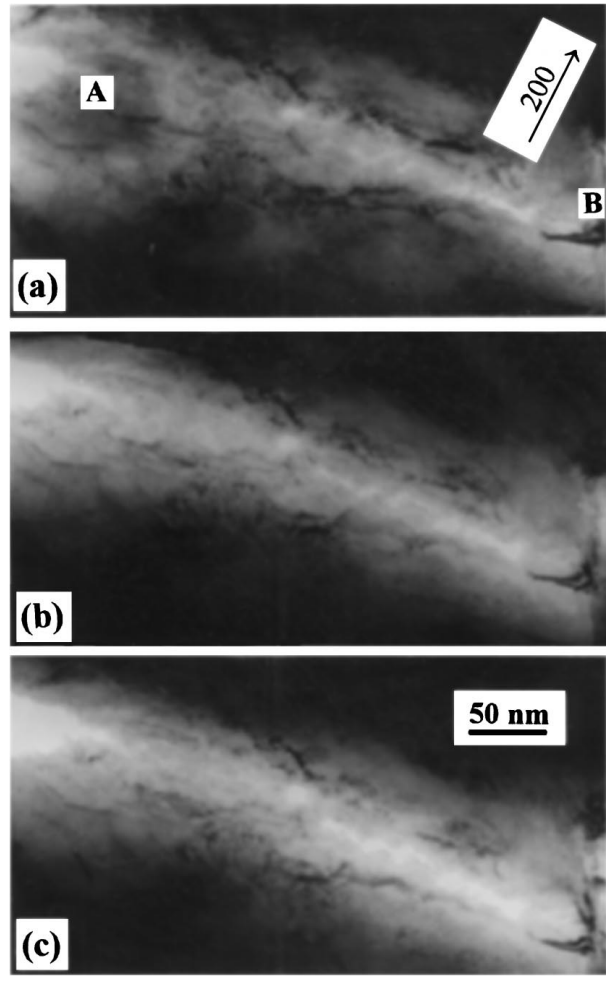

Figure 1 The microvoid formation under constant displacement in the hydrogen-free specimen. BD ~ 0 1 1, **g** = 200.

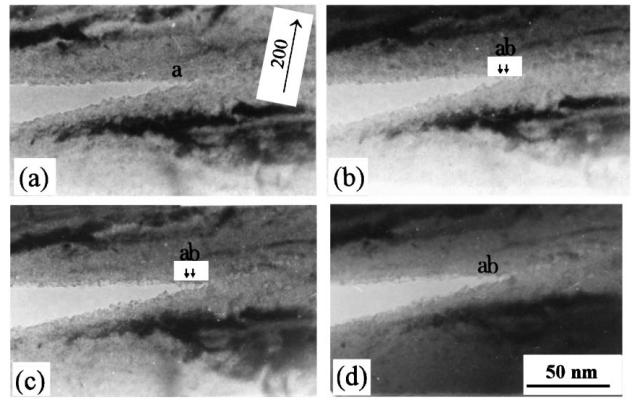

Figure 2 Two nanovoids formed just ahead of the crack tip after keeping constant displacement for a long time in the hydrogen-free specimen. BD ~ 0 1 1, **g** = 200.

3.2. Crack initiation in the hydrogenated specimen with high C_H

Fig. 3 shows the HIC procedure within the first five min when the hydrogen concentration is not less than 100 ppm, according to Appendix A. There are two salient phenomena different from the cracking in the hydrogen-free specimen. First, the foil became pockmarked after loading. The bright specked contrast is not voids because they did not show the expected contrast variation as the objective focus was changed from under to over focus. The *in situ* elongation indicated that these bright specks formed after the foil was loaded. Since the exact loaded position was not recognized before observing the pockmarking phenomenon, the *in situ* comparison between before and after tension could not be realized. Hence the formation procedure of the bright specks was not grasped. In addition, they developed

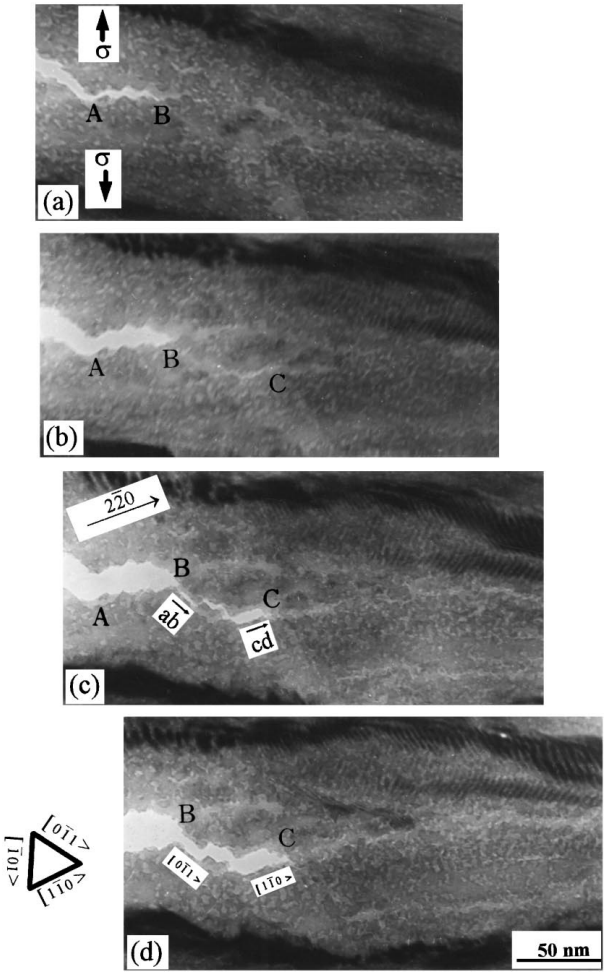

Figure 3 Cleavage cracking took place in the heavily hydrogenated specimen when C_H was high. BD $\sim$ 1 1 1, $\mathbf{g}$ = 2 $\bar{2}$ 0.

too quickly to take photos when C_H was high. It is conceivable that small C_H will slow down this development appreciably, (see Fig. 5). The *in situ* inspection indicated that local breakage of the surfaces, which led to local thinning of the specimen, is responsible for these bright speckles. The breakage might be caused by the inner nanovoids near the surfaces. The similar procedure also happened in hydrogen-free specimens if only saturated vacancies could initiate nanovoids. In this case, the distribution of light spots is certainly much sparser than that in the hydrogenated specimen [Fig. 2]. Second, the cracking was brittle. By inspection, it can be seen from length AB in Fig. 3a and length BC in 3c that the directions of microcrack propagation are ***ab*** and ***cd***. The crack propagated along the two directions alternately, leading to quasi-cleavage fractographic morphology (e.g. length AB). During the propagation from Fig. 3c to Fig. 3d, microcracks (i.e., AB and CD) did not blunt into voids, which is the important nature of brittle cracking. The previous work [15, 20] showed that the behavior of microcracks after their nucleation was principally different between ductile and brittle fractures. Microcracks blunted into voids, resulting in ductile propagation. Otherwise microcracks cleaved continuously, leading to brittle propagation. Cottrell [21] pointed that the growth of microcracks after their nucleation was a critical stage between ductile and brittle fracture. If the stress for the growth of microcracks

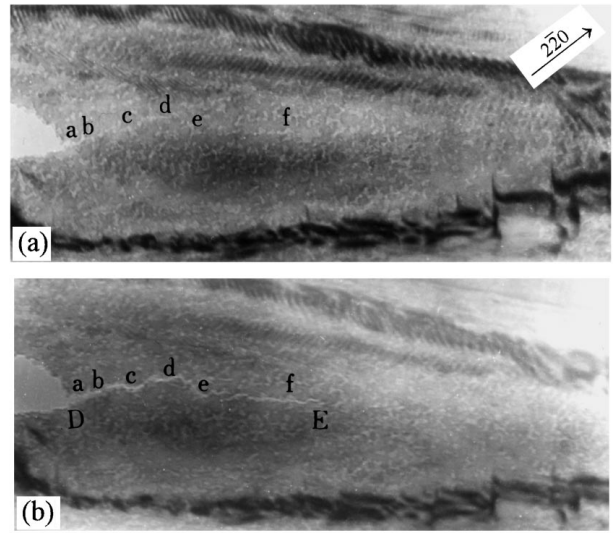

Figure 4 Brittle cracking took place in the heavily hydrogenated specimen when C_H was high. BD $\sim$ 1 1 1, $\mathbf{g}$ = 2 $\bar{2}$ 0.

is smaller than the yield stress, the fracture is brittle. Otherwise, the fracture is ductile. In Fig. 3, the microcracks formed under lower stresses than the yield stress, with the assistance of hydrogen. They could also propagate under similar stresses, instead of blunting into voids that is a plastic procedure driven by the yield stress.

The foil normal is near [1 1 1], which is also the approximate beam direction of Fig. 3 with operating vector $\mathbf{g} = [2\ \bar{2}\ 0]$. By trace-analyzing Fig. 3c, the direction ***ab*** is consistent with the cross line [0 1 1] between plane (1 1 1) and (1 $\bar{1}$ $\bar{1}$), and ***cd*** with the cross line [1 1 0] between plane (1 1 1) and ($\bar{1}$ 1 1). This fact indicates that, at least in 310 stainless steel with high C_H, HIC develops through alternative cleavage of two different {1 1 1} planes, which results in quasi-cleavage fractographic morphology. The Burgers vector of the dislocations at the top of the figures was determined to be $\pm\frac{1}{2}[1\,0\,\bar{1}]$. These dislocations were bowing to the moving direction. Referencing to the triangle of three $\langle 1\,1\,0\rangle$ on (1 1 1) plane, it can be seen from Fig. 3c that these dislocations are roughly screw.

Fig. 4 demonstrates the cracking that happened after Fig. 3. The HIC was also brittle. However no obvious crystallographic cleavage was observed. By inspection, it can be seen that there are the traces of crack DE in Fig. 4a, as marked with "abcdef". That is to say crack DE in Fig. 4b developed from some bright spots in Fig. 4a, which were frail positions of cracking.

3.3. Crack initiation in the hydrogenated specimen with low C_H

As mentioned above, the development of light spots could be caught when C_H was reduced during the elongation of the specimen in TEM. The cracking shown in Fig. 5 happened after loading the same specimen again and keeping constant displacement, or no further development was observed. Comparing Fig. 5a with 5d, it can be seen that the originally clean area ABC was spotted with some light spots. A void *a* was forming in

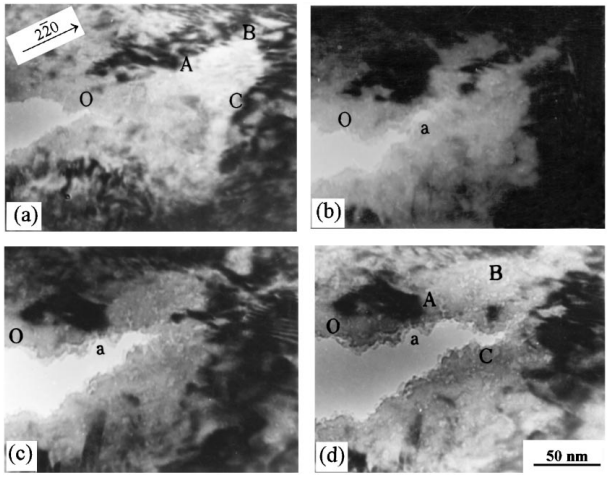

Figure 5 Hydrogen-enhanced ductile cracking through nanovoid nucleating, growing into microvoids and connecting with each other when C_H was low. BD $\sim$ 1 1 1, **g** = 2 $\bar{2}$ 0.

Fig. 5b, and it connected with the main crack in Fig. 5c, resulting in the dimple morphology on the crack edge in Fig. 5d. After keeping constant displacement for a long time (e.g. more than 30 m), there was insufficient hydrogen to cause much of the effect, and the failure procedure was very similar to that of the hydrogen-free specimen.

Finally, two points should be emphasized. First, the hydrogen atoms were in the hydrogenated specimen before tension because no bubble was observed before tension, and the cracking demonstrated hydrogen-free characteristics after the hydrogenated foil was placed in the air for long enough time before tension. This result agrees with others' work [12]. Second, what is investigated in the present paper is nanovoids that were induced by vacancies and hydrogen without involving plastic deformation. Their role in fracture is naturally different from that of the voids (or microvoids), a role that was discussed by many works [5, 11], where voids were produced by plastic deformation. The presence of the nanovoids increases brittle tendency. The microvoids, however, enhance ductility.

4. Discussion

4.1. Hydrogen-induced nanovoids

Both of the equilibrium concentrations of vacancies and hydrogen will increase with the local stress concentration σ_{yy}, as given in [22, 16]

$$C_V(\sigma) = C_{V0}\, exp\left(\frac{\sigma_{yy} b^3}{kT}\right) \tag{1}$$

and

$$C_H(\sigma) = C_{H0}\, exp\left(\frac{\overline{V_H}\sigma_h}{RT}\right) \tag{2}$$

where $\overline{V_H}$ is the partial mole volume of hydrogen in the alloy, and $\sigma_h = \frac{1}{3}(\sigma_{xx} + \sigma_{yy} + \sigma_{zz})$.

The ratio $C_V(\sigma)/C_{V0}$ was estimated to be 10^{14} in the DFZs ahead of a loaded crack tip, a ratio which corresponds to the concentration of the supersaturation vacancies under high temperature of 800–900 °C in absence of the stress concentration [15]. Using the similar estimation, $C_H(\sigma)/C_{H0}$ is evaluated to be 37 when $\overline{V_H} = 10^{-6}\ m^3/mol$ [23] (no value of $\overline{V_H}$ is available in γ-Fe, so the magnitude order of $\overline{V_H}$ in α-Fe is adopted here), $\sigma_h = 9 \times 10^9\ N/m^2$ in the DFZ [24] and $T = 300$ K. In the case of large hydrogen concentrations, more superabundant vacancies would form near the crack tip [17, 18]. The highly supersaturated vacancies tend to form clusters and even nanovoids. At the same time, the heavily supersaturated hydrogen is liable to combine with vacancy clusters or unstable voids, and hence to initiate nanovoids. The critical size of a stable void r_c is given by [15]

$$r_c = [8\Gamma]\left[4\sigma_{yy} + \frac{3\sigma_{yy}^2}{E}\right]^{-1} \tag{3}$$

where Γ is the true surface energy of the material and E is Young's module. Choosing $\Gamma = 2$ J/m^2[25], $\sigma_{yy} = 9 \times 10^9\ N/m^2$ in the DFZ [24], it was obtained that $r_c \approx 0.5$ nm [15]. This result indicates that heavy concentration of tensile stress largely reduces the critical size of void nucleation.

In the case of hydrogen, the critical size of a stable void r_c(H) is given by

$$r_c(\mathrm{H}) = [8\Gamma(\mathrm{H})]\left[4\left(\sigma_{yy} + p_{H_2}\right) + \frac{3\left(\sigma_{yy} + p_{H_2}\right)^2}{E}\right]^{-1} \tag{4}$$

where $\Gamma(\mathrm{H}) < \Gamma$. Equation 4 indicates clearly that hydrogen further reduces the minimum size of nanovoid nucleation. Γ(H) is estimated as follows: Adopting a simple coordination model and considering the nearest interaction, atomic binding energy $E_b = z(\frac{\phi}{2})$, where ϕ is the bond energy that is shared by a pair of closest atoms, and z is the coordination number. Some of the coordination bonds are broken so as to produce two surfaces. Supposing that z_0 coordination bonds are broken to form a surface atom and interatomic spacing is a in the surface, it is obtained that $a^2\Gamma = z_0(\frac{\phi}{2}) = \frac{z_0}{z}E_b$. Since $\Gamma \propto E_b$, $\Delta\Gamma/\Gamma = \Delta E_b/E_b$. Hsiao and Chu [26] obtained experimentally that atomic binding energy E_b was reduced 5% by 1% (atom) hydrogen. Hence, $|\Delta\Gamma/\Gamma|$ is estimated to be almost 100% when $C_H(\sigma)/C_{H0} = 37$ in the DFZ, $C_{H0} = 100$ ppm and then $C_H(\sigma) = 21\%$ (atom). Therefore, r_c became almost zero in the case of saturated hydrogen. The instant impression is that the reduction seems absolutely absurd. But subsequent thinking indicates it has some plausability. Hydrogen atoms combine to form molecular hydrogen as soon as they enter the vacancy clusters or unstable nanovoids. The reaction is irreversible. Hence, no matter how small they are, nanovoids will become stable if only there is molecular hydrogen in them. In principle, the critical size of a stable void r_c could be reduced to H_2 volume. In a word, highly saturated hydrogen strongly

reduces the critical size of a stable void r_c though the amazing reduction is clearly over-estimated. There are several factors responsible for the over estimation. Firstly and mainly, the result—that atomic binding energy E_b was reduced 5% by 1% (atom) hydrogen—was obtained according to line extrapolation, which might be over-evaluated. Secondly, the magnitude order of $\underline{V_H}$ in α-Fe was adopted. Thirdly, the derivation of Equation 3 [15] does not fit such a small nanovoid. For a very small volume medium, the concepts of surface energy and volume energy are ambiguous.

p_{H_2} is evaluated as follow. According to Arrhenius equation, it is obtained that

$$\ln C_H = \ln A(p_{H_2})^{1/2} - \left(\frac{\Delta H}{R}\right)\frac{1}{T}. \qquad (5)$$

In 18-8 stainless steel [27], it was determined that $\ln A = 1.314$ and $\Delta H/R = 366.9$ (the units of C_H and p_{H_2} are 10^{-3} cm^3/100 g and mmHg respectively). Supposing T = 300 K and $C_H = 3700$ ppm $= 4.144 \times 10^6$ ($\times 10^{-3}$ cm^3/100 g), we obtain $p_{H_2} \approx 157$ mmHg $= 2 \times 10^4$ N/m^2, which is much smaller than the stress 9×10^9 N/m^2 in the DFZ although p_{H_2} has been, in fact, over-evaluated because C_H should have been a hydrogen concentration in perfect lattice rather than the apparent value. In a word, hydrogen pressure, even of so highly saturated hydrogen, will not cause much of the effect on nanovoid nucleation.

The above estimation suggested that hydrogen reduced the critical size of the stable nanovoid mainly through decreasing the surface energy rather than increasing the hydrogen pressure.

In summary, vacancies and hydrogen atoms migrate to the region of sufficiently concentrated tensile stresses ahead of the crack tip, resulting in superabundant vacancies and hydrogen there. These supersaturated vacancies tend to form an amount of vacancy clusters which combine with hydrogen and become stable to form a lot of nanovoids randomly near the crak tip. The burst of nanovoids at the foil surfaces results in the specked morphology.

4.2. Hydrogen-induced cracking

Undoubtedly, hydrogen concentration is the critical factor of HIC in stainless steels. The present work showed that a sufficiently high concentration of hydrogen induced cleavage on a nano-scale, which corresponds to quasi-cleavage on a macro scale. And low hydrogen concentration enhanced ductile cracking. The aim of this section is to discuss the micromechanism of hydrogen-inducing cleavage along {1 1 1} planes and that of hydrogen-enhancing ductile fracture.

No obvious reason can be conceived why hydrogen atoms tend to distribute along {1 1 1} planes in the perfect and stress-free structure. The cleavage microcracks can be initiated by applied stresses along suitably orientated crystal planes. However, this view cannot explain the fact demonstrated in Fig. 3, where $(\bar{1}\,\bar{1}\,1)$ and $(1\,\bar{1}\,\bar{1})$ are not the most suitably orientated planes. The pressing situation of interstitial hydrogen atoms can be relaxed by defects, such as vacancies and dislocations. Our first thoughts are that hydrogen tends to combine with vacancy clusters that are produced randomly in highly concentrated stress fields so as to initiate nanovoids. This model, however, cannot explain Fig. 3 either.

It is well known that in the equilibrium distribution about an edge dislocation, there is an increased concentration of vacancies but a decreased concentration of interstitials in the region of compression; the opposite holds for the region of tension [28]. When a slip system is activated by the applied force, the corresponding dislocations break away from the point-defect atmospheres (including core drags) and glide along the {1 1 1} planes, leaving the defect clusters along the {1 1 1} planes. The vacancy clusters and hydrogen clusters tend to combine to produce stable nanovoids along the {1 1 1} planes. Thus linkage between {1 1 1} planes is weakened by these nanovoids.

Since C_H and C_V are both high enough in the DFZ ahead of a loaded crack, the nanovoids are very dense. When the apparent, i.e., average, stress on the honeycomblike plane is low, the real stresses on the linkage parts can be up to cohesive strength. Hence the residual atomic bonds between the {1 1 1} planes can break under low apparent applied force. i.e., cleavage happens. In addition, in the case of low applied force, only one or two slip systems are activated. Thus the density of nanovoids on each activated {1 1 1} slip plane is larger than in the case of multislipping (ductile behavior). This factor further increases the brittle tendency described above. Therefore the term *cleavage*, which means the break of atomic bonds, is not strictly used here because the present cracking involves nanovoids unlike the cleavage of intrinsically brittle materials.

With the releasing of hydrogen, fewer and fewer nanovoids form. Hence greater and greater force is needed to break the linkage parts between {1 1 1} planes. Of course, the real strength of breaking residual atomic bonds does not change. The greater applied force will cause multislipping, which further reduces the average density of nanovoids along each {1 1 1} plane and blunt microcracks into microvoids. Therefore the microvoids can grow largely before they meet each other. The coarse voids, together with the multislipping, resulted in the dimple fractography of ductile fracture (Fig. 5). In the case of hydrogen-enhanced ductile failure, the mechanism of randomly distributed nanovoids should also operate.

In summary, vacancy clusters and hydrogen atom clusters are left along {1 1 1} planes when the corresponding slip systems are activated. Vacancy clusters and hydrogen atoms tend to combine with each other to form stable nanovoids. When C_H is high and applied force is low, very dense nanovoids are produced, and then HIC takes place along {1 1 1} planes. Otherwise, in the case of low C_H and high applied stresses, sparse nanovoids nucleate and grow into microvoids. The connection between microvoids results in ductile fracture.

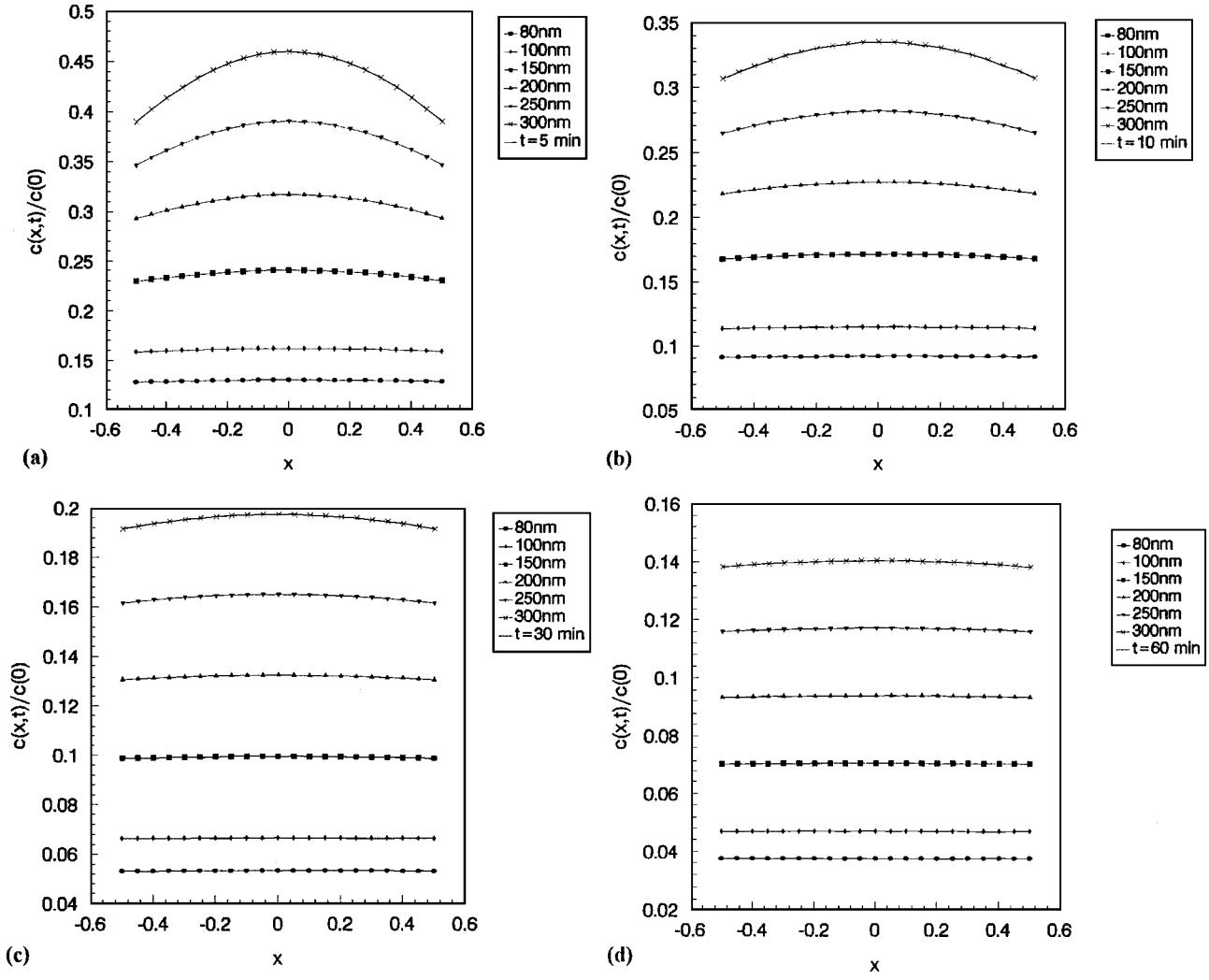

Figure A1 $C_H(x, t)/C_0$ curves of different sample thicknesses for different lengths of time.

5. Conclusions

1. The effect of hydrogen on cracking can be investigated successfully in stable austenite stainless steels that are hydrogenated heavily.

2. When C_H is high, HIC happens through nanovoid nucleation and then cleavage along {1 1 1} planes. In the case of low C_H, hydrogen enhances ductile fracture through hydrogen-induced microvoid nucleation, growth and connection.

3. The model for HIC is proposed in the paper. Vacancies and hydrogen atoms migrate to the region of tensile stress concentration ahead of the crack tip, resulting in supersaturated vacancies and hydrogen there. First, these supersaturated vacancies tend to form an amount of vacancy clusters that combine with hydrogen and become stable nanovoids randomly near the crack tip. Second, dislocations break away from defect atmospheres and move away from the DFZ, leaving vacancy and hydrogen clusters along {1 1 1} planes. Hydrogen tends to combine with vacancy clusters and initiate nanovoids along {1 1 1} planes. Dense nanovoids connect each other along {1 1 1} planes before growing, resulting in brittle cracking. Scattered nanovoids grow into microvoids through plastic relaxation, leading to ductile fracture.

Appendix A

Suppose the thickness of the thin foil is a constant l and the original hydrogen concentration $C_H = C_0$. The x-axis is along the foil normal, and its origin is fixed at the mid-thickness of the specimen. The solution of Fick's second law that satisfy the initial condition

$$C_H(x, 0) = \begin{cases} C_0 & \left(|x| \le \frac{l}{2}\right) \\ 0 & \left(|x| > \frac{l}{2}\right) \end{cases}$$

is

$$C(x, t) = \frac{C_0}{2}\left[\operatorname{erf}\left(\frac{x + \frac{l}{2}}{2(Dt)^{1/2}}\right) - \operatorname{erf}\left(\frac{x - \frac{l}{2}}{2(Dt)^{1/2}}\right)\right] \tag{A1}$$

Figure A1 shows $C(x, t)/C_0$ after 5, 10, 30 and 60 m, where l equals 80, 100, 150, 200, 250 and 300 nm. Suppose $C_0 = 200$ ppm, it can be seen that C_H is about 25 ppm in the specimen with thickness of $200 \sim 250$ nm after 1 h. Experimentally, the hydrogen concentration

was measured, by degassing at 1000 °C, to be more than 200 ppm after cathodically charging for 50 h. It reduced to about 50 ppm after observation in TEM for 60 m. The difference between the experimental measure and the theoretical estimation is mainly due to many hydrogen traps in the specimen.

For the specimen in this paper, its thickness was about 200 nm by convergent-beam-electron-diffraction (CBED), and the original hydrogen concentration was about 200 ppm. According to Equation A1, the hydrogen concentration should have reduced to about 60 ppm. Considering hydrogen traps, however, it can be kept to 100 ppm.

Acknowledgement

The authors acknowledge the support to this research project by the National Nature Science Foundation of China.

References

1. T. D. LEE, T. GOIDENBERG and J. P. HIRTH, *Metall. Trans.* **10A** (1979) 199.
2. R. A. ORIANI and P. H. JOSEPHIC, *Acta metall.* **27** (1979) 997.
3. T. D. LEE and I. M. BERNSTEIN, *Acta metall. mater.* **39** (1991) 363.
4. J. P. HIRTH, in "Hydrogen Effects on Material Behavior," edited by A. W. Thompson (TMS-AIME, 1990) 677.
5. X. G. JIANG, W. Y. CHU and J. M. XIAO, *Acta metall. mater.* **43** (1995) 3727.
6. I. G. PARK and A. W. THOMPSON, *Metall. Trans.* **21A** (1990) 465.
7. R. GARBER, I. M. BERNSTEIN and A. W. THOMPSON, *Scripta metall.* **10** (1976) 341.
8. R. GARBER, I. M. BERNSTEIN and A. W. THOMPSON, *Metall. Trans.* **12A** (1981) 225.
9. DONG- IL KWON and R. J. ASARO, *Acta Metall. Mater.* **38** (1990) 1595.
10. H. G. F. WILSDORF, *Mater. Sci. Eng.* **59** (1983) 1.
11. A. M. CUITIÑO and M. ORTIZ, *Acta Metall. Mater.* **44** (1996) 427.
12. W. Y. CHU, J. YAO and C. M. HSIAO, *Metall. Trans.* **15A** (1984) 729.
13. D. ELIEZER, *Met. Trans.* **10A** (1979) 935.
14. D. P. ABRAHAM and C. J. ALTSTETTER, *Metall. Mater. Trans.* **26A** (1995) 2859.
15. Q. Z. CHEN, W. Y. CHU, Y. B. WANG and C. M. HSIAO, *Acta Metall. Mater.* **43** (1995) 4371.
16. J. O. M. BOCKRIS and P. K. SUBRAMANYAM, *Acta Metall.* **19** (1971) 1205.
17. R. B. MCLELLAN and Z. R. XU, *Scripta Metall. Mater.* **36** (1997) 1201.
18. V. G. GAVRILJUK, V. N. BUGAEV and Y. N. PETROV, *et al. Scripta Metall. Mater.* **34** (1996) 903.
19. E. RIECKE, in "Hydrogen Effects in Metals," edited by I. M. Bernstein and A. W. Thompson (AIME, 1981) 77.
20. K. W. GAO, Q. Z. CHEN, W. Y. CHU and C. M. HSIAO, *J. Mater. Sci. Tech.* **11** (1995) 31.
21. A. H. COTTRELL, in "Fracture" (John Wiley, New York, 1959) 20.
22. J. FRIEDEL, in "Dislocation" (Pergamon, Oxford, 1964) 312.
23. J. P. HIRTH, *Metall. Trans.* **11A** (1980) 861.
24. T. ZHU, W. YANG and T. GUO, *Acta. Metall. Mater.*, **44** (1996) 3049.
25. A. W. THOMPSON and J. F. KNOTT, *Metall. Trans.* **24A** (1993) 523.
26. C. M. HSIAO and W. Y. CHU, in "Hydrogen Effects in Metals," edited by I. M. Bernstein and A. W. Thompson, (AIME, 1981) 255.
27. M. SMIALOWSKI, in "Hydrogen in Steel" (Pergamon, Oxford, 1962) 45.
28. J. P. HIRTH and J. LOTHE, in "Theory of Dislocations" 2nd ed. (A Wiley-Interscience Publication, New York, 1982) 503.

Received 22 November 1997
and accepted 15 July 1998